PHYSICAL REVIEW B VOLUME 3, NUMBER 6 15 MARCH 1971

Photoelectron Energy Spectra and the Band Structures of the Noble Metals

Neville V. Smith
Bell Telephone Laboratories, Murray Hill, New Jersey 07974
(Received 15 October 1970)

Photoelectron energy distributions and their second derivatives have been measured on Cu, Ag, and Au in the photon energy range 4.0–11.4 eV. Samples were prepared by evaporation in ultrahigh vacuum and were coated with an approximate monolayer of Cs or Na in order to lower the work function. The experimental energy spectra show much new structure, and in each metal there are instances of behavior indicative of direct transitions from the *d* bands. The predictions of the direct-transition model have been calculated by performing numerical evaluations of the energy distribution of the joint density of states (EDJDOS) using interpolated band structures. Energy locations of structure in the experimental spectra are compared with peak loci in the theoretical EDJDOS. The agreement is found to be good for Cu and Ag, and reasonable (in view of the nonrelativistic nature of the calculations) for Au. Calculations of the density of states and the interband joint density of states are also presented, and the latter are compared with experimental values for ϵ_2.

I. INTRODUCTION

Photoemission has emerged as a powerful method for determining the band structure of solids. The usefulness of the technique in metals was demonstrated by Berglund and Spicer[1] in their pioneering experiments on Cu and Ag. While their spectra revealed the location of the *d* bands in a new and spectacular way, Berglund and Spicer found that they could not completely reconcile their results with the conventional theory of direct ($\vec{k}$-conserving) transitions. This has contributed to the proposal of nondirect transitions in some materials.[2] More recent experiments[3–5] have revealed the direct-transition effects. This paper reports the results of extensive measurements and calculations of the photoelectron energy spectra on Cu, Ag, and Au. An interpretation will be attempted in terms of direct transitions.

The work has proceeded along two parallel courses, one experimental and the other theoretical. The experimental work has consisted of measuring the photoelectron energy spectra on samples of Cu, Ag, and Au whose work functions had been lowered by applying an approximate monolayer of Cs or Na to the surface. Measurements were also performed on the clean surfaces prior to cesiation or sodiation; these reproduced the results of other workers[6] and will not be discussed in detail here. It has been found in this work,[3] and in other laboratories,[4] that it is possible to cesiate samples with much less distortion and less obliteration of spectral structure than in earlier experiments. The successful cesiation and sodiation of Au has been particularly gratifying in view of the severe alloying problem which can occur with this metal.[7]

Another development in the experiments was the use of higher-derivative spectra. It was found that measurements of the second derivative of the photoelectron energy distribution revealed structure not discernible in the energy distribution itself.[8] The combination of the two techniques – (i) cesiation or sodiation to lower the work function and (ii) measurement of higher-derivative spectra, to improve the resolution – has uncovered much new information.

The theoretical side of the work has consisted of performing numerical calculations with model band structures. A detailed calculation of the exact shape and magnitude of the energy distribution of photoemitted electrons would be difficult since the photoemission process is quite complicated and involves knowledge of electron-electron scattering strengths, momentum matrix elements, optical-absorption depths, transport and escape considerations, surface phenomena, etc. We have therefore contented ourselves with calculations of the energy distribution of the joint density of states (EDJDOS). This is a simple property of the band structure with which we can meaningfully compare the experimental spectra. It is determined entirely by the E-k dispersion relations. We therefore avoid making assumptions concerning the details of the photoemission process. We do, however, make one very important assumption, namely, that there exists a *volume contribution* to the photocurrent in which electrons are optically excited within the interior of the material and then escape without scattering. This assumption does seem to have been substantiated experimentally.[9] The k-space integrations involved in the evaluation of the EDJDOS necessitate the use of an interpolation scheme. The details of the numerical calculations are described and illustrated in Sec. II using Cu as the prime example.

In Secs. IV and V, we compare the energy locations of structure in the experimental spectra with peaks in the theoretical EDJDOS. Our emphasis in both theory and experiment will therefore be on peak

positions. In this respect, and also in the use of higher-derivative spectra, our approach resembles that used in modulated optical-absorption studies.[10] There, the first line of attack in interpretation is to assign structure in the modulated spectra to analytic singularities in the joint density of states (JDOS). The distinction in photoemission studies is that we will be working in terms of the *energy distribution* of the joint density of states (EDJDOS). It is this capability of providing information on both the energies and the frequencies of optical transitions which gives the photoemission technique its extra power.

II. PHOTOEMISSION AND BAND STRUCTURE

A. Energy Distribution of Joint Density of States

In conventional theory, optical interband transitions are direct in the sense that they can occur only between states with the same reduced $\vec{k}$ vector. If $\mathcal{E}_i(\vec{k})$ and $\mathcal{E}_f(\vec{k})$ represent the electron energies in an initial band i and a final band f, and if $\hbar\omega$ is the photon energy, optical transitions are restricted to a surface in k space of constant interband energy difference given by

$$\Omega_{fi}(\vec{k}) = \mathcal{E}_f(\vec{k}) - \mathcal{E}_i(\vec{k}) - \hbar\omega = 0 . \tag{1}$$

An important quantity is the JDOS defined by

$$\mathcal{J}(\hbar\omega) = (2\pi)^{-3} \sum_{f,i} \int' d^3k\, \delta(\Omega_{fi}(\vec{k})) . \tag{2}$$

The prime on the integral sign indicates that the range of integration is restricted to those portions of k space for which $\mathcal{E}_f > E_F > \mathcal{E}_i$, where E_F is the Fermi energy. The summation is performed over all pairs of bands (i, f) which can participate. The JDOS therefore represents the total number of direct transitions which can take place at the frequency $\hbar\omega$. If we wish to connect with any experimentally observable quantity, we should weight each transition with an appropriate strength factor given by $|\vec{P}_{fi}|^2$, the square of the momentum matrix element. The interband contribution to the imaginary part of the dielectric constant ϵ_2 is given by the well-known expression[11]

$$\omega^2\epsilon_2 = \frac{e^2\hbar^2}{3\pi m^2} \sum_{f,i} \int' d^3k\, |\vec{P}_{fi}|^2 \delta(\Omega_{fi}(\vec{k})) . \tag{3}$$

In what follows, however, we will adopt a constant-matrix-element approximation in which each transition is treated with equal weight. In this approximation, the JDOS is a measure of the total number of photoexcited electrons at frequency $\hbar\omega$.

In photoemission experiments, we are interested in not just the number of photoelectrons but also their energy spectrum. A property of the band structure which we require is the EDJDOS defined by

$$\mathfrak{D}(\mathcal{E}, \hbar\omega) = (2\pi)^{-3} \sum_{f,i} \int' d^3k\, \delta(\Omega_{fi}) \delta(\mathcal{E} - \mathcal{E}_i(\vec{k})) . \tag{4}$$

The extra δ function picks out the direct transitions from a specific initial energy $\mathcal{E}$. The EDJDOS represents the energy distribution of photoexcited electrons referred to initial states. Strictly speaking, each transition should be weighted by $|\vec{P}_{fi}|^2$ if we wish to connect with the true photoelectron spectrum, but we will remain within the constant-matrix-element approximation. This has the advantage of making calculations very straightforward since $\mathfrak{D}(\mathcal{E}, \hbar\omega)$ is a property solely of the E-k dispersion relations and requires no knowledge of the actual wave functions.

Another quantity of interest is the usual density of states (DOS) defined by

$$\rho(\mathcal{E}) = (2\pi)^{-3} \sum_{i} \int d^3k\, \delta(\mathcal{E} - \mathcal{E}_i(\vec{k})) . \tag{5}$$

The interrelationships among the various densities of states which we have introduced are immediately apparent from their definitions. The EDJDOS bears a resemblance to the DOS, the main difference being the inclusion of the extra δ function $\delta(\Omega_{fi})$. It is useful to think of the EDJDOS as the density of states over the surface of constant interband energy difference, a surface which shifts to a new position in k space on changing the photon energy. Measurements of the photoelectron energy spectra should give fine-grained information on the band structure since we are, in essence, sampling the density of states over a succession of different slices through k space. The information is potentially richer than that contained in the DOS, which is the density of states over the whole Brillouin zone.

B. Interpolated Band Structures

The integrals defined above have been evaluated numerically by a histogram technique which involves sampling points in k space arranged along a very dense mesh. The calculation requires a method for generating the energy eigenvalues $\mathcal{E}_i(\vec{k})$ and $\mathcal{E}_f(\vec{k})$ at general points in the Brillouin zone. Moreover, the method must be quite fast since a great many points have to be visited in order to accumulate sufficiently large statistical samples. The combined interpolation schemes devised recently for d-band metals meet these requirements very well. The scheme adopted here is that due to Hodges, Ehrenreich, and Lang,[12] although the similar scheme due to Mueller[13] would serve just as well. The procedure consists of setting up the elements of a 9×9 Hamiltonian matrix composed of a 4×4 orthogonalized plane wave (OPW) and a 5×5 tight-binding d Hamiltonian in the diagonal blocks; terms in the off-diagonal blocks simulate the effects of hybridization. Diagonalization of the model Hamiltonian provides a fast and convenient way of generating the

energy eigenvalues throughout the whole zone.

The procedure has been to fit the interpolation scheme to the results of reliable band calculations taken from the published literature. A choice arises as to whose band calculation we shall fit the parameters, and so we have been guided by the following four empirical criteria.

(i) The depth of the uppermost d band below the Fermi level should be 2.1, 4.0, and 2.5 eV, respectively, in Cu, Ag, and Au. These values are known from the edge in experimental ϵ_2 data[14–16] and are confirmed by photoemission spectra.

(ii) The width of the d bands should be 3.2, 3.5, and 5.7 eV in Cu, Ag, and Au, respectively. These values are known from other photoemission experiments[5] and are confirmed by the work described below.

(iii) The level $L_{2'}$ must lie a few tenths of an eV below the Fermi level in order to bring about the well-established necking of the Fermi surface with the hexagonal face of the Brillouin zone.

(iv) The $L_{2'} - L_1$ band gap is known from optical studies to be about 4 eV in each metal,[15,16] a value which is confirmed by photoemission spectra.

In the case of Cu, the choice was quite easy. The bands obtained in the APW calculation by Burdick[17] satisfy all four criteria. We therefore used the fit to Burdick's bands proposed by Hodges *et al.*[12] without any changes.

The situation in Ag and Au is not as good. Band theorists have experienced difficulty in producing results which satisfy criterion (i). Recent calculations have incorporated an element of empiricism. For example, Snow[18] has been able to locate the top of the d bands correctly by using $\frac{5}{6}$ of the conventional Slater exchange. A similar approach has been adopted by Ballinger and Marshall,[19] who have published band structures for both Ag and Au. Ballinger and Marshall's bands satisfy criteria (ii) and (iii) very well and are also quite good for criterion (i). We have therefore used Ballinger and Marshall's bands as the starting point of our fitting procedure.

In both Ag and Au, the d-band levels of Ballinger and Marshall were left untouched, thus preserving agreement with criterion (ii). The Fermi levels were adjusted by a few tenths of an eV to secure better agreement with criterion (i). In Ag, the levels $L_{2'}$, $X_{4'}$, and L_{12} were given minor adjustments so as to restore agreement with criterion (iii) while maintaining agreement with criterion (iv). In Au, the level L_{12} was lowered to improve agreement with criterion (iv) and restore agreement with criterion (iii).

The interpolation scheme was fitted to the adjusted Ag and Au band structures outlined above using a prescription proposed by Hodges.[20] Further details of the parameters are to be found in the Appendix. Figure 1 shows the resulting interpolated band structures plotted for the ΓX direction. These are the band structures used in the numerical calculations reported below. It is recognized that these interpolated bands have their limitations. First, the interpolation scheme is nonrelativistic. This could lead to particularly severe errors in the base of Au where the spin-orbit splitting is known to be large. Mueller *et al.*[21] have shown that combined interpolation schemes can be modified to accommodate relativistic effects, but such modifications have not been included here. A second limitation concerns the behavior of the bands at high energies. We will be concerned with optical transitions to final states 11 eV above the Fermi level. These states are well removed from the d-band region and are determined largely by the four-OPW portion of the Hamiltonian. It is highly doubtful whether four OPW's are sufficient and an inspection of Burdick's original bands, for example, reveals that the interpolation scheme does indeed go astray at these high energies. A certain amount of latitude should be allowed when it comes to comparing the predictions of these band structures to experiment.

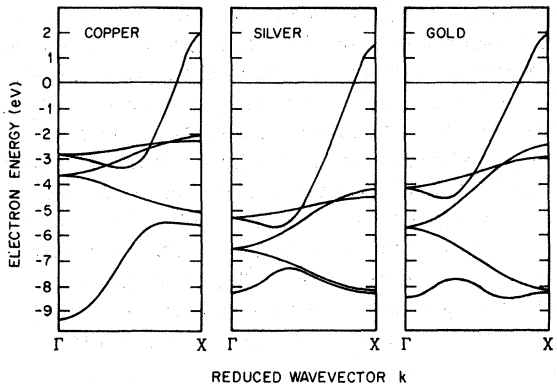

FIG. 1. Energy band structures of Cu, Ag, and Au in the ΓX direction calculated from the interpolation scheme.

C. Numerical Results

The JDOS, EDJDOS, and DOS were computed by a histogram technique similar to that used by Brust[22] on Si and by Koyama and Smith[23] on Al. A total of 375 000 points arranged on a cubic mesh in the irreducible $\frac{1}{48}$ of the Brillouin zone were sampled. At 12 000 of these points, the energy eigenvalues were determined by diagonalization of the model-Hamiltonian matrix. The eigenvalues at the other points were determined by linear interpolation.

The photon energy and electron energy scales had been divided into intervals, thus creating a set of "bins" to be used for keeping running scores of the optical transitions. The counting procedure was to scan through k space along the points of the mesh. At each point, the energy eigenvalues were calculated. The permitted optical transitions were

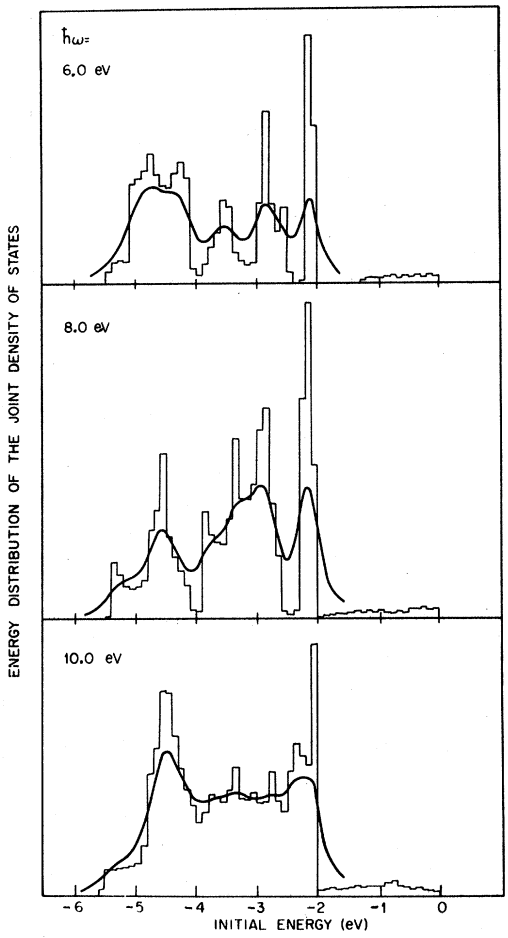

FIG. 2. Histograms of the EDJDOS for Cu at three different photon energies. The smooth curves were obtained by including a 0.3-eV Lorentzian broadening. The EDJDOS is referred to the energies of the initial states in the optical transitions, taking the zero at the Fermi level.

deduced and then dumped into the appropriate bins. At the end of the scan, histograms for the EDJDOS were constructed from the contents of the bins. The DOS was computed in a similar fashion.

The histograms for the EDJDOS in Cu are shown for three widely spaced photon energies in Fig. 2. The main features are a set of prominent peaks extending from -2.0 to -5.5 eV. (The Fermi level is taken as zero on the energy scale.) These peaks are due to transitions from the d bands. At the lower photon energies, the peaks are sharp and well separated. With better resolution, these peaks would possibly reveal themselves to be of the logarithmic singularity variety discussed by Kane.[24] Note that the profile of the EDJDOS changes quite markedly on varying the photon energy. This is a consequence of the restrictive nature of the k-space sampling imposed by the energy and wave-vector conservation rules. The EDJDOS represents the density of states over a surface in k space which shifts its position on changing $\hbar\omega$.

The smooth curves also shown in Fig. 2 were obtained by convolving the histograms with a Lorentzian broadening function whose width at half-maximum was 0.3 eV. The broadening illustrates the possible effects of lifetime broadening and finite instrumental resolution. By multiplying these curves by an appropriate escape function, it is possible to arrive at a quantitative prediction for the energy spectrum of externally emitted photoelectrons. Such curves have been calculated and have proved quite successful in comparisons with the experimental spectra for both clean[25] and cesiated[3] Cu. These calculations, however, assume that the photoemission process is exclusively a volume effect. Recent theoretical work indicates that surface contributions could be important.[26] In view of this and other likely distorting effects, such calculations will not be repeated here. The emphasis in this paper will be on *structure* in the EDJDOS, its existence and energy location.

A convenient way in which to summarize large numbers of histograms such as those shown in Fig. 2 is to construct the structure plot shown in Fig. 3. The smooth curves represent the energy locations of peaks in the EDJDOS. The full curves represent strong peaks and the broken curves represent weaker peaks. The distinction is arbitrary but serves to illustrate the relative strengths of the peaks and the variation in strength with photon energy.

We draw particular attention to the region for which $-3.9 < \delta < -2.6$ eV and $6.5 < \hbar\omega < 8.5$ eV indicated by the dotted rectangle in Fig. 3. The interweaving and crisscrossing of the curves in this region is once again a consequence of the $\vec{k}$-conser-

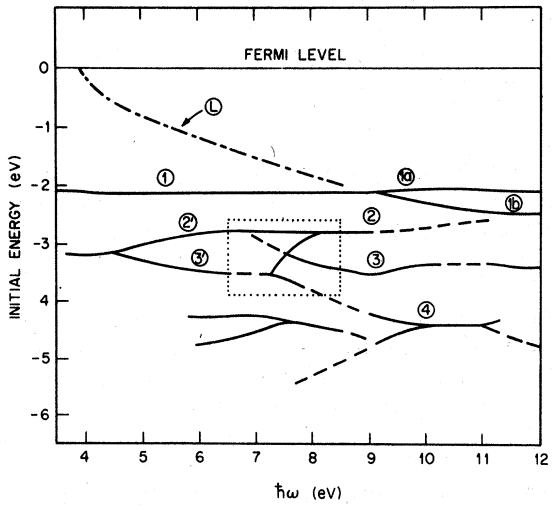

FIG. 3. Structure plot of the energy location of peaks in the EDJDOS of Cu.

vation selection rule. It will be seen in Sec. IV that this behavior can be seen quite clearly in the experimental spectra and provides one of the most conclusive indications if direct transitions in d-band metals.

For photon energies greater than about 9 eV, the curves in Fig. 3 remain approximately horizontal. This implies that peaks in the photoelectron spectrum are predicted to remain stationary when referred to initial-state energy. Alternatively, when referred to final-state energy (i.e., the energy with which the photoelectrons actually emerge from the metal), a given peak will advance in energy on changing $\hbar\omega$ by an amount equal to the increment in $\hbar\omega$. Such equal-increment behavior has been taken as strong[2] (although not complete[27]) evidence that $\vec{k}$ conservation is unimportant. However, it is apparent from Fig. 3 and from the calculations of the EDC's reported by Smith and Spicer[25] that equal-increment behavior in Cu is not a serious obstacle to a direct-transition interpretation.[28]

The line labeled L in Fig. 3 differs from the other curves in that it represents an edge rather than a peak in the EDJDOS. It corresponds to the low-energy limit for conduction-band-to-conduction-band transitions. These start in the vicinity of $L_2' \rightarrow L_1$ and then spread to other parts of the zone on increasing $\hbar\omega$. At low photon energies, the contribution to the EDJDOS from the conduction-band-to-conduction-band transitions is distinct and can be seen as the rectangular-box-shaped contribution with a low-energy edge at -1.3 eV in the histogram for $\hbar\omega = 6.0$ eV in Fig. 2. In fact, the rectangular-box shape can be understood in terms of a simple two-band model discussed by Koyama and Smith.[23] The characteristic square shape for the low-energy edge arises from one of the three kinds of singularities in the EDJDOS discussed by Kane.[24] Evidence of this edge was seen in the early experiments by Berglund and Spicer[1] on Cu and Ag. It has also been seen in Au, and the behavior in the three metals will be compared in Sec. V.

D. ϵ_2 and Joint Density of States

The JDOS was generated as a by-product of the calculations for the EDJDOS, since it follows from the definitions above that

$$\mathcal{J}(\hbar\omega) = \int d\mathcal{E}\, \mathfrak{D}(\mathcal{E}, \hbar\omega) \ . \tag{6}$$

In other words, the JDOS is simply the area under the EDJDOS histogram. It follows also from Eq. (3) that, in a constant-matrix-element approximation, ϵ_2 is proportional to the JDOS; we have

$$\epsilon_2 \propto \mathcal{J}(\hbar\omega)/\omega^2 \ . \tag{7}$$

The histograms obtained for $\mathcal{J}(\hbar\omega)/\omega^2$ are shown in Fig. 4, where they are compared with the experimental values of ϵ_2 taken from a recent paper by

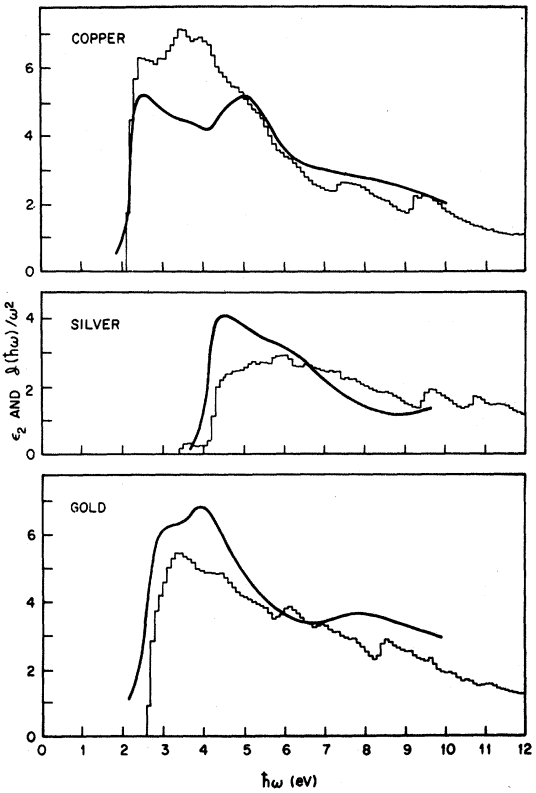

FIG. 4. Comparison of the experimental ϵ_2 with $\mathcal{J}(\hbar\omega)/\omega^2$ for Cu, Ag, and Au. The vertical scales correspond to the units of ϵ_2; the theoretical histograms contain an arbitrary scaling factor (but which is the same for each metal).

Beaglehole and Erlbach.[16] The edge in ϵ_2 is reproduced reasonably well, which is not surprising since the edge was used in fitting the optimum depth of the d bands in the model band structures. The relative strength of pieces of structure in ϵ_2 is not well reproduced, and the discrepancy presumably lies in the assumption of constant matrix elements.

The comparison in Fig. 4 gives us an estimate of the adequacy of the constant-matrix-element approximation. For example, in Cu there are two main peaks in ϵ_2 at 2.5 and 5.0 eV. The 2.5-eV peak is due to transitions from the uppermost d band, and the bulk of the 5.0-eV peak is now generally attributed to transitions from the lowermost d bands.[11,29,30] The values of $\mathcal{J}(\hbar\omega)/\omega^2$, however, show a large intensity between these peaks, indicating that the constant-matrix-element approximation tends to overestimate the relative strength of transitions from the intermediate d bands. Calculations of ϵ_2 which include the effects of matrix elements have been attempted by Mueller and Phillips[11] and by Dresselhaus.[29] While the matrix elements are shown to vary considerably across the zone, the agreement with experiment obtained by these authors is barely better than that shown in Fig. 4.

E. Discussion

Several valid criticisms can be leveled at the attempt outlined above to relate photoemission energy spectra and band structure. These are now discussed and it will be argued that some of the objections can be sidestepped by confining one's attention to the energy location of structure in the spectra and deferring the problem of peak strengths and shapes for further study.

The most conspicuous defect is the assumption of constant matrix elements. Calculations by Mueller and Phillips[11] indicate that the matrix-element variations are quite considerable. The effect on the relative heights of peaks in the photoelectron spectra will be more severe than in ϵ_2 since the latter is an integrated quantity [Eq. (3)] and the variations have an opportunity to average themselves out. However, the calculated matrix elements[11] seem to vary smoothly with $\vec{k}$, and it is difficult to see how they could produce fresh structure. It is suggested that the worst effects will be the occasional suppression of a peak when the matrix elements vanish completely.

Another problem which we have ignored is the transport of the photoexcited electron to the surface and its escape across it. Attempting to be a little more precise than in Eq. (4), the energy distribution of photo*emitted* electrons $\mathfrak{N}(\mathcal{E}, \hbar\omega)$ should be written as follows[22]:

$$\mathfrak{N}(\mathcal{E}, \hbar\omega) = C \sum_{i,f} \int' d^3k\, \delta(\Omega_{fi}(\vec{k}))\, \delta(\mathcal{E} - \mathcal{E}_i(\vec{k})) \times |\vec{P}_{fi}|^2 T(\mathcal{E}_f, \vec{k}) , \quad (8)$$

where C is a normalization factor and $T(\mathcal{E}_f, \vec{k})$ is an escape function which incorporates the probabilities of the electron reaching the surface and escaping. It is possible to integrate over the δ functions to obtain

$$\mathfrak{N}(\mathcal{E}, \hbar\omega) = C \sum_{f,i} \int \frac{dl_{fi}}{|\nabla_k \mathcal{E}_f \times \nabla_k \mathcal{E}_i|} |\vec{P}_{fi}|^2 T(\mathcal{E}_f, \vec{k}) . \quad (9)$$

The line integral is performed round the line of intersection of the constant energy surfaces given by $\mathcal{E}_i = \mathcal{E}$ and $\mathcal{E}_f = \mathcal{E} + \hbar\omega$. In simple theory,[1] the escape function $T(\mathcal{E}_f, \vec{k})$ contains the factor αl, where α is the optical-absorption coefficient and l is the hot-electron mean free path. The mean free path may in turn be expressed as $\tau |\nabla_k \mathcal{E}_f| / \hbar$, the product of a scattering time and a group velocity. Making the substitutions into Eq. (9), we see that the factor $\nabla_k \mathcal{E}_f$ will appear in both the numerator and the denominator of the integrand. The partial cancellation can bring about a suppression of structure in the EDJDOS; the magnitude of the effect has been considered by Janak *et al.*[28] and by Kane.[31] Calculation of $T(\mathcal{E}_f, \vec{k})$ should also take account of crystal orientation. Mahan[32] has shown that such angular considerations can cause additional distortion from the EDJDOS. A common approximation, however, is to replace $T(\mathcal{E}_f, \vec{k})$ by some averaged escape function which can then be taken outside the integral.

In the foregoing discussion, the photoemission process has been treated as a completely volume effect. Recent theoretical developments[26,33] have revived the view that the surface photoelectric mechanisms may provide a contribution. The notion that the volume process occurs in three sequential steps – (i) optical excitation, (ii) transport to the surface, and (iii) escape – has also come under question.[33]

III. EXPERIMENTAL DETAILS

A. Measurement Technique

The experimental photoelectron energy spectra reported here were measured by the modulated retarding potential technique using a cylindrical geometry.[34] The method consists of applying retarding voltages to a collector electrode and superimposing a small ac sine voltage. The first harmonic of the ac component of the photocurrent is proportional to dI/dV, the first derivative of the curve of photocurrent I vs retarding voltage V; $-dI/dV$ is in turn proportional to the energy distribution curve (EDC) of photoemitted electrons.

An advantage of the ac technique is the ability to measure derivatives of the EDC by tuning in on the higher harmonics.[8,35] Much of the interpretation in this paper will be based on curves of d^3I/dV^3 which were measured by synchronously detecting the third harmonic of the ac photocurrent. The d^3I/dV^3-vs-V curve represents the negative of the *second* derivative of the EDC. Results for $-dI/dV$ and d^3I/dV^3 obtained on cesiated Cu at a photon energy of 7.8 eV are shown in Fig. 5. The sign of the third-derivative curve was chosen so that regions of high negative curvature in the EDC (i.e., peaks and shoulders) come out as peaks in the higher-derivative curve. This peak-for-peak (and valley-for-valley) correspondence makes measurements of d^3I/dV^3 (and odd harmonics) easier to interpret by eye than measurements of d^2I/dV^2 (and higher even harmonics). The sign inversion in the d^3I/dV^3 spectra will be maintained throughout this paper. It is seen that in the higher-derivative curve, the effect has been to pick off the structure and eliminate the background. More important than this, we note that the higher-derivative curve has revealed new structure. For example, the rather broad single peak in the 2.2–3.5 voltage range shown in Fig. 5 has been resolved into a closely spaced quadruplet (three peaks and a shoulder). The reasons for the higher resolution and the details of the measuring technique will be discussed elsewhere.[36] We attribute the structure in the photo-

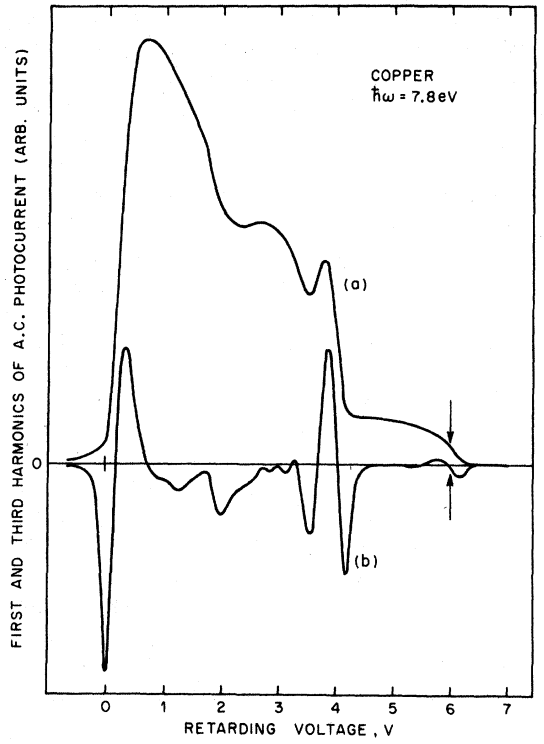

FIG. 5. Photoelectron energy spectra measured on cesiated Cu at $\hbar\omega = 7.8$ eV. Curve (a) is the amplitude of the first harmonic and corresponds to $-dI/dV$ and the photoelectron energy distribution; curve (b) is the amplitude of the third harmonic corresponding to d^3I/dV^3, the negative of the second derivative of the energy distribution. [Curves (a) and (b) have different vertical scales.] The vertical arrows represent the estimated location of the Einstein cutoff.

electron energy spectra to singularities in the EDJDOS. The derivatives of the spectrum are expected to be large at the singularities. In this respect, the higher-derivative technique bears a close resemblance to the modulation techniques used in optical-absorption studies.[10]

Locating the high-energy cutoff of the EDC poses the following minor problem. The work function $e\varphi$ of the sample used in Fig. 5 was measured by means of a Fowler plot and found to be 1.8 eV. According to the well-known Einstein relation, the maximum kinetic energy with which a photoelectron can emerge is given by $\hbar\omega - e\varphi$, which equals 6.0 eV. The measured energy distribution is two- or three-tenths of an eV wider than this, due presumably to instrumental broadening effects. Where, then, is the true high-energy edge? Since the inside of the collector was of the same material (cesiated Cu) as the sample, the work functions are identical, which means that the zero of retarding voltage coincides with the zero of kinetic energy. In a recent analysis of the broadening factors in the retarding potential method, DiStefano and Pierce[37] concluded that the geometrical distorting effects become more severe at the high-energy end of the EDC. Following a suggestion by Eastman,[38] we regard the zero end of the EDC as the most reliable and then measure out an exact $\hbar\omega - e\varphi$ eV along the horizontal scale and locate the Einstein maximum at the point indicated by the vertical arrows in Fig. 5. Note that this location coincides with where the d^3I/dV^3 curve passes through zero. This is just what one would expect if there was a well-defined edge in the true (i.e., unbroadened) EDC.

The method used for locating the Einstein maximum described above has been used consistently throughout the work described in this paper. Some workers prefer to use the point where the EDC meets the horizontal axis, or the point where the straight portion of the leading slope would cross the axis if it were produced. The various choices account for some of the differences which the reader will encounter in the literature. For example, we now place the uppermost d peak in Cu at 2.15 eV below the Fermi level, which is closer than the value of 2.3 eV quoted previously by the author[3,25] and by other workers.[6] Another example is the case of Au. In this work, we locate the uppermost d peak in the EDC at about 2.5 eV below the Fermi level. This agrees with the position found by Eastman and Cashion,[5] who used the same method for locating the Einstein maximum.[38] We therefore locate the Au d bands marginally closer to the Fermi level than the 2.6 eV quoted by Nilsson *et al.*,[4,39] and significantly closer than the 3.0 eV quoted by Krolikowski and Spicer.[6]

Use of the higher-derivative spectra can also cause slight changes in the energy location of peaks. In Fig. 5, the uppermost d-band peak in the d^3I/dV^3 curve (retarding voltage ~3.9) occurs at a slightly higher energy than the corresponding peak in the $-dI/dV$ curve. The peak positions in the higher-derivative curves are regarded as a better indication of the true positions of singularities in the EDJDOS than the peaks in the EDC.

The spectra shown in Fig. 5 show a large peak within 1 eV of the low-energy end. This is attributed to photoexcited electrons which have undergone an inelastic electron-electron scattering but are sufficiently energetic to escape from the metal. Berglund and Spicer[1] demonstrated that a peak of just this kind is to be expected. The scattering peak is not directly related to band structure and will therefore be ignored in the interpretation which follows.

B. Sample Preparation

The samples of Cu, Ag, and Au were prepared by evaporation from tungsten filaments in an ultra-high-vacuum system in which the typical operating pressure was 10^{-10} Torr. Photoemission measure-

ments were taken on the clean metals and the shapes of the EDC's were found to be in agreement with the most reliable previous measurements.[5,6,39] The samples were then cesiated by a method described before.[3,40] Glass ampules containing cesium sealed under vacuum had been placed in the chamber and kept intact during the pumpdown and bakeout procedure. The ampules were cracked open inside the vacuum chamber, and the cesiation performed by gentle heating of the ampule. Only sparing amounts were used and it was found possible to lower the work functions of the samples without the smearing and distortion of the EDC's which often accompanies cesiation. Fresh samples of the noble metal could be prepared by further evaporations from the tungsten filament. On one of the pumpdowns, all three of the noble metals were investigated by use of multiple filaments.

In the case of Au, a different set of measurements were performed in which sodium was used in place of cesium. The problem with Au is the strong possibility of alloying[7] with Cs. Although our findings have confirmed those of Nilsson *et al.*[4,39] that it is possible to avoid alloying by careful cesiation, it seemed desirable to run some experiments with a metal other than cesium. If the results are unaffected, then we have further confidence that alloying has been avoided. Figure 6 shows the photoelectron energy distributions taken at $\hbar\omega = 10.2$ eV on various clean, cesiated, and sodiated surfaces of Au. We also show the second derivative of the EDC taken on cesiated Au. All the curves have been plotted against $E - \hbar\omega + e\varphi$, where E is the kinetic energy in vacuum. This choice of scale refers the electrons to their initial states and places the zero of energy at the Fermi level. The important point to notice is the consistency in the energy location of structure. There are six pieces of structure in the d-band region labeled 1–6; these correspond, respectively, to peaks B–G observed by Nilsson *et al.*[4]

Ideally, the only effect of cesiation or sodiation should be to lower the work function. If this were the case in practice, we would expect a detailed correspondence between the structure in clean, cesiated, and sodiated samples. It can be seen that the spectra in Fig. 6 do satisfy this criterion, indicating that the structure is characteristic of pure Au. The correspondence test was applied wherever possible between clean and cesiated spectra.

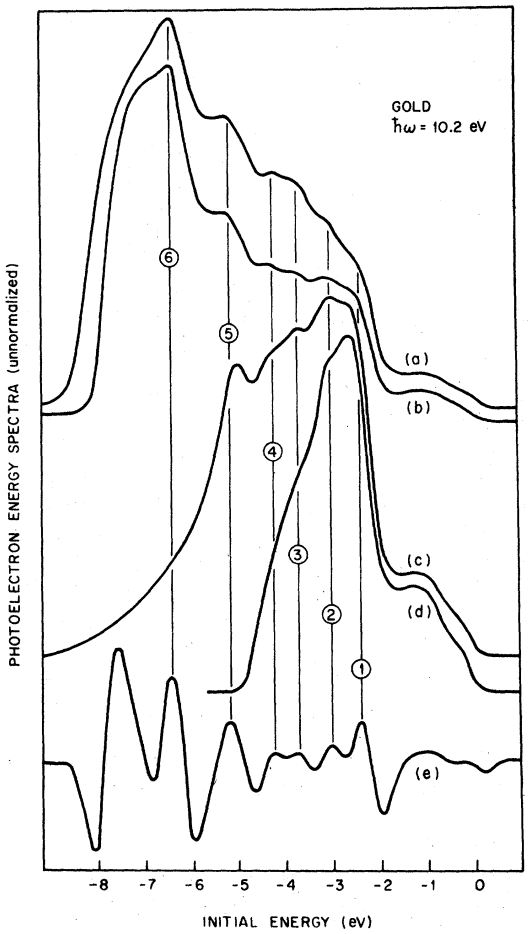

FIG. 6. Photoelectron energy spectra at $\hbar\omega = 10.2$ eV taken on various samples of Au; (a) EDC on fully sodiated Au; (b) EDC on fully cesiated Au; (c) EDC on partially sodiated Au; (d) EDC on clean Au; (e) negative of the second derivative of the EDC on fully cesiated Au.

IV. TRANSITIONS FROM d BANDS

A. Copper

The experimental photoelectron EDC's obtained on cesiated Cu are shown in Fig. 7 for a range of photon energies where the d bands are being exposed. The curves are plotted against $E - \hbar\omega + e\varphi$, which refers the photoelectrons to their initial states and places the zero of energy at the Fermi level.

There is a feature of the spectra in Fig. 7, which is highly characteristic of direct transitions. The doublet consisting of peaks 2′ and 3′ at $\hbar\omega = 6.5$ eV undergoes a marked change on increasing $\hbar\omega$. Peak 3′ fades away while peak 2′ broadens to become a single peak at $\hbar\omega = 7.8$ eV. This single peak then splits into the doublet labeled 2 and 3. It has been shown[3] that this doublet-singlet-doublet sequence is reproduced quite well in theoretical calculations of the EDC's from the broadened EDJDOS discussed in Sec. II C. These profile changes were obscured in the experimental EDC's of Berglund and Spicer[1] by a large peak in the middle of the d-band region. Comparison with EDC's on clean Cu has shown[40] that the obscuring peak in Berglund and Spicer's data is probably spurious. The structure in their EDC's does not completely match the struc-

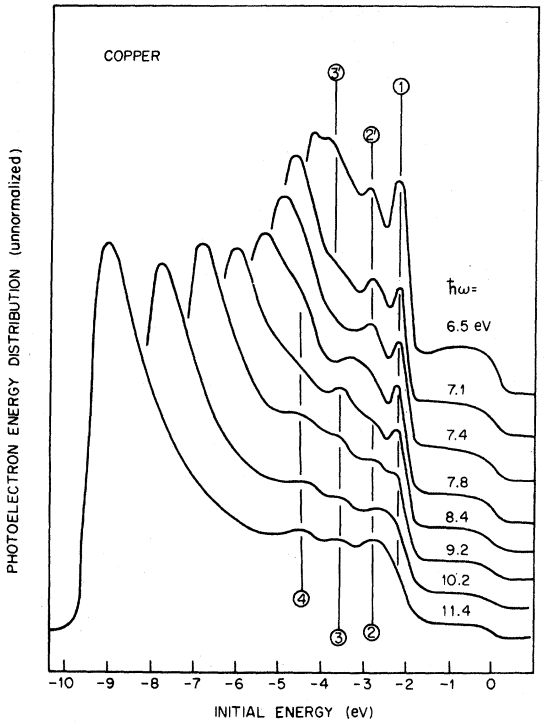

FIG. 7. Photoelectron energy distributions measured on cesiated Cu referred to initial-state energy.

ture in the clean Cu EDC's in the regions where comparison is possible. The new EDC's presented here, on the other hand, satisfy this correspondence criterion quite well. It is conjectured that the spurious peak in Berglund and Spicer's data is an effect of alloying between the Cu and the Cs.

Notice also that the EDC's in Fig. 7 show no evidence of the peak observed by Berglund and Spicer[1] at − 6 to − 7 eV. This anomalous peak has been the subject of some speculation and has been attributed, among other things, to an unanticipated peak in the Cu density of states. The peak finds its way into the optical density of states proposed by Krolikowski and Spicer.[6] It has been found in this work that the anomalous peak does sometimes appear in samples which have been excessively cesiated. Similar effects have been reported by Callcott and MacRae[41] in their work on Ni. It appears, therefore, that the anomalous peaks, when they occur, are associated with the Cs and do not represent an intrinsic property of the underlying metal.

A selection of the second-derivative spectra taken on cesiated Cu is shown in Fig. 8. The same structural features can be seen as were observed in Fig. 7. The greater resolution of the derivative technique enables us to see new features. For example, the doublet 2′ + 3′ once again evolves into the doublet 2 + 3 but the intermediate stages are now seen to be more complicated. Clearly, the photon energy range 7.4–8.4 eV is of great interest and it has been investigated more intensively. The results are illustrated in Fig. 9, where we show the second-derivative spectra at very close intervals of $\hbar\omega$. The profile changes are quite rapid. The peak labeled 2′ is observed to split into a doublet on increasing $\hbar\omega$. A further splitting gives rise to the quadruplet at $\hbar\omega = 7.8$ eV (three peaks plus a shoulder representing the remains of peak 3′). On increasing $\hbar\omega$ further, the quadruplet eventually evolves into the doublet 2 + 3. The sequence of events in the electron energy range − 3.9 to − 2.5 eV is doublet-triplet-quadruplet-triplet-doublet, which is much richer than the doublet-singlet-doublet sequence observed with the lower resolution of the regular EDC's in Fig. 7. Note that this interesting behavior occurs in the energy range singled out for special attention in Sec. IIC and indicated by the dotted rectangle in Fig. 3. Indeed, the numbering of the peaks in the experimental spectra of Figs. 7–9 was chosen so as to match the numbering of the EDJDOS peak loci plotted in Fig. 3.

Theory and experiment are summarized and compared for a wide range of photon energies in the structure plot shown in Fig. 10. The smooth curves represent the loci of peaks in the d-band region of the theoretical EDJDOS; these curves are identical to those shown in Fig. 3. The full circles represent the energy locations of peaks in experi-

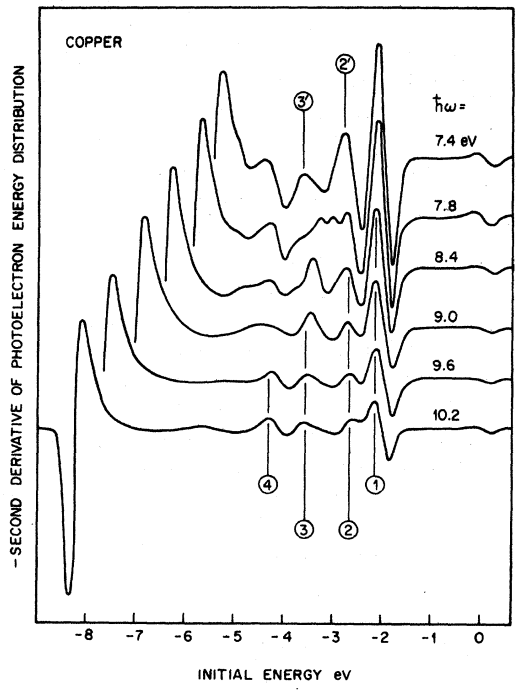

FIG. 8. Second derivative (minus) of the photoelectron energy distribution measured on cesiated Cu.

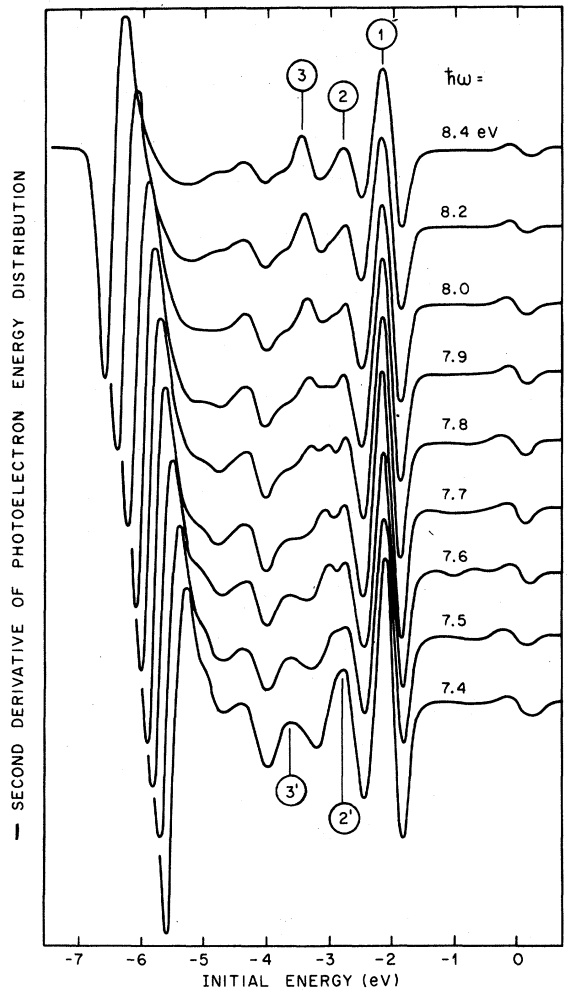

FIG. 9. Second derivative (minus) of the photoelectron energy distribution measured on cesiated Cu at closely spaced intervals of photon energy between 7.4 and 8.4 eV.

mental photoelectron spectra such as those shown in Figs. 8 and 9; the open circles represent weaker peaks or shoulders. The large peak at the extreme low-energy end of the spectra has been omitted from this plot since it is an artifact of scattering and escape considerations and is not directly related to band structure. The agreement between theory and experiment is seen to be remarkably good. In particular, the interweaving and crisscrossing of the theoretical curves match quite well with the pronounced spectral profile changes of Fig. 9.

Agreement could be improved by shifting the entire network of theoretical curves in Fig. 10 several tenths of an eV to the right. This suggests that our model band structure places the upper bands slightly too low. Arbitrarily raising the final-state bands by several tenths of an eV would lead to much the same pattern for the peak loci, but, since the transitions at any given point in k space would now occur at higher photon energies, the main effect would be an approximately rigid shift of the pattern to the right. It would be straightforward to make the necessary adjustments to the interpolation scheme, but this has not been attempted here. On the contrary, it should be emphasized that the interpolation scheme parameters used here were those proposed by Hodges *et al.*[12,20] with no changes whatsoever. The excellence of the agreement in Fig. 10 therefore speaks well for the reliability of Burdick's bands and the interpolation scheme.

The open circles in the bottom right-hand corner of Fig. 10 correspond to the broad weak peak observable at about − 6 eV in the spectrum at $\hbar\omega = 10.2$ eV shown in Fig. 8. This does not seem to be related to the band structure of Cu, and is possibly a vestige of the "anomalous" peak discussed above.

B. Silver

Photoelectron energy distributions measured on cesiated Ag are shown in Fig. 11. These curves are similar to those measured by Berglund and Spicer,[1] although the sharpness of structure is slightly better. At the highest photon energies, five pieces of structure labeled 1–5 can be seen. Peaks 1–4 have been observed previously in the work of Walldén[42] on partially cesiated Ag. Peak 1 is due to transitions from the uppermost d band. Walldén places this peak at 4.5 eV below the Fermi level; in our work we place it between 4.0 and 4.2 eV below the Fermi level. The difference possibly arises through the different methods for locating the Einstein maximum mentioned in Sec. III A.

At the lowest photon energy shown in Fig. 11,

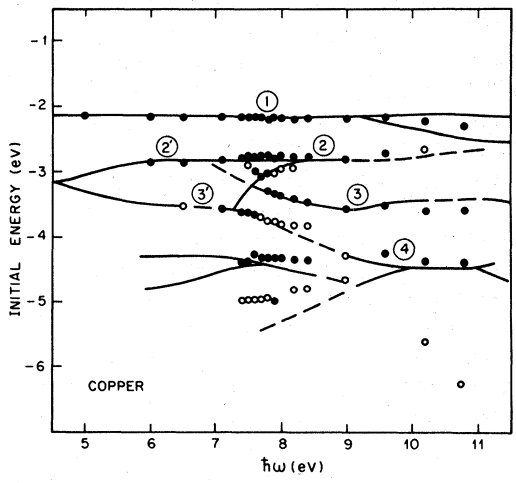

FIG. 10. Structure plot for Cu comparing peak positions in the experimental spectra (full and open circles) with peak loci in the theoretical EDJDOS (smooth curves).

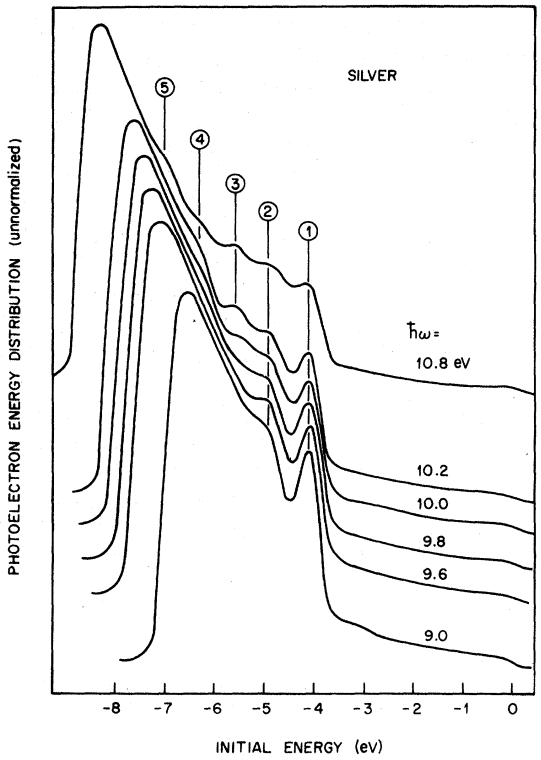

FIG. 11. Photoelectron energy distributions measured on cesiated Ag referred to initial-state energy.

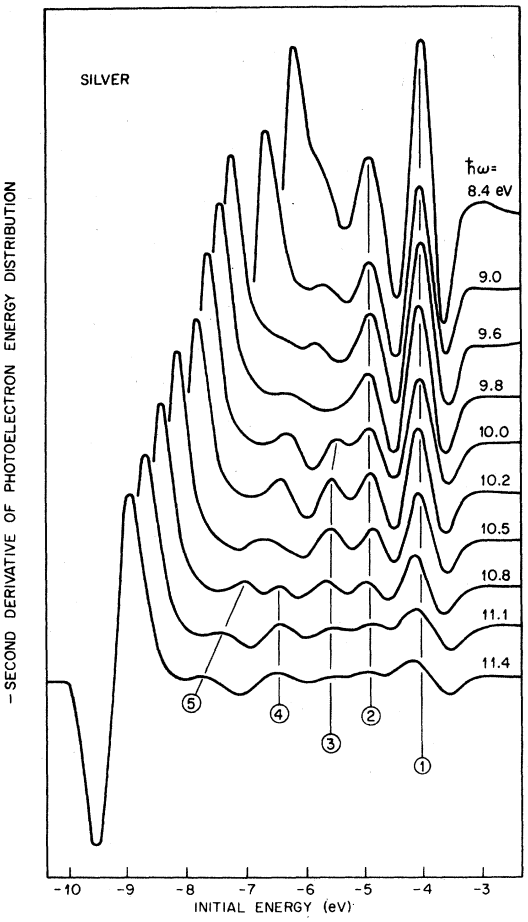

FIG. 12. Second derivative (minus) of the photoelectron energy distribution measured on cesiated Ag.

there is no sign of peak 3. This peak emerges somewhere between $\hbar\omega = 9.8$ and 10.0 eV. The abrupt emergence of a peak is a characteristic effect of the direct nature of optical transitions. The behavior is seen much more clearly in the second-derivative spectra illustrated in Fig. 12. The abrupt emergence of peak 3 between $\hbar\omega = 9.8$ and 10.0 eV is unmistakable.

Theory and experiment are summarized and compared in the structure plot shown in Fig. 13. The smooth curves are loci of peaks in the theoretical EDJDOS calculated from the interpolated band structure based on Ballinger and Marshall's band[19] as described in Sec. II B. The full and open circles are the locations of structure in the experimental spectra. At the high photon energies the path of each of the experimental peaks 1 to 5 falls close to one of the theoretical curves with which it can therefore be identified. Notice also that the theoretical peak 3 is predicted to split off from peak 2 just below $\hbar\omega = 10$ eV. There are parts of the structure plot where theory and experiment diverge; however, the over-all agreement seems to be very good.

Calculations of the EDJDOS were also performed after fitting the interpolation scheme to Snow's band calculation of Ag using $\frac{5}{6}$ of the Slater exchange.[18] The peak loci predicted by this EDJDOS were also in qualitative agreement with experiment; in particular, peak 3 was still predicted to split off from peak 2. The width of Snow's Ag d bands was somewhat narrower than that observed in the experiment-

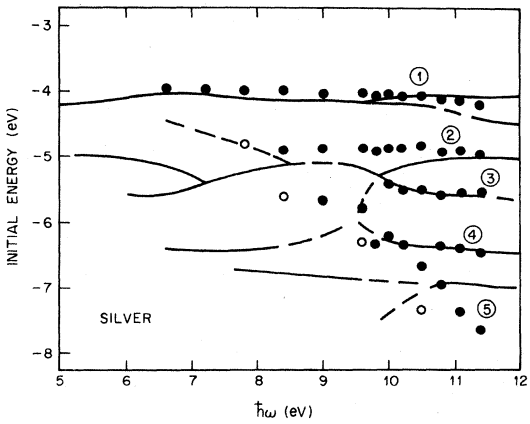

FIG. 13. Structure plot for Ag comparing peak positions in the experimental spectra (full and open circles) with peak loci in the theoretical EDJDOS (smooth curves).

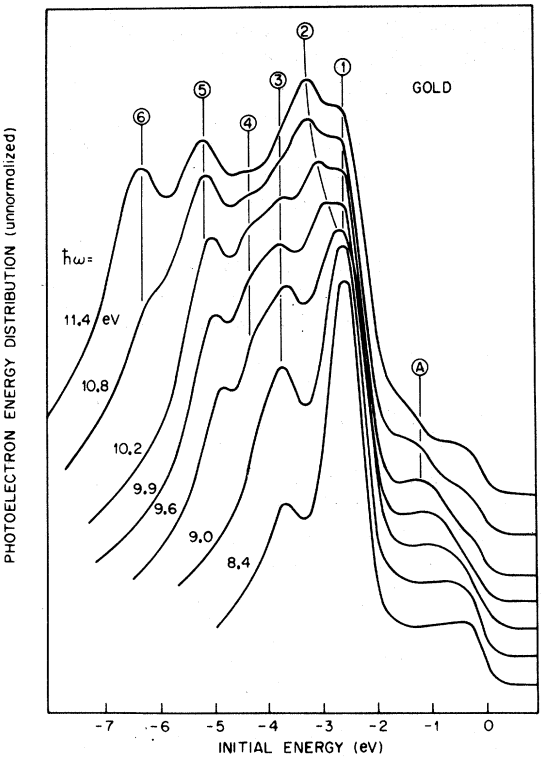

FIG. 14. Photoelectron energy distributions measured on partially sodiated Au referred to initial-state energy.

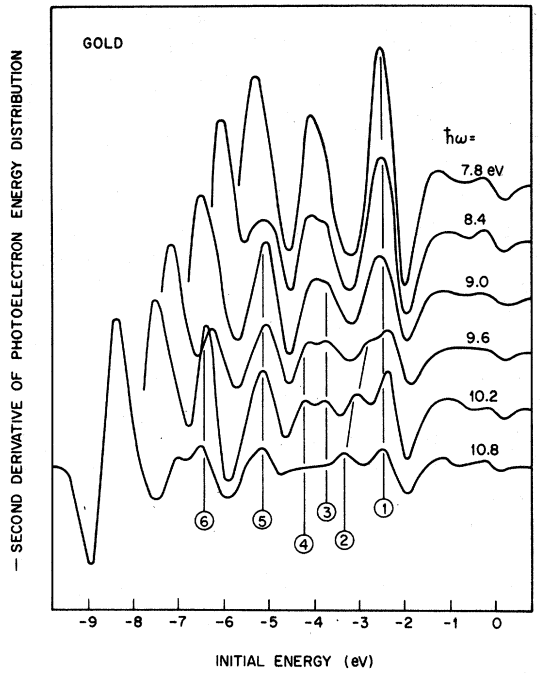

FIG. 15. Second derivative (minus) of the photoelectron energy distribution measured on fully cesiated Au.

al spectra. Ballinger and Marshall's bands give the correct width, and so we regard them as marginally superior.

C. Gold

Photoelectron energy distributions measured on partially sodiated Au are shown in Fig. 14. There are six principal pieces of structure labeled 1–6 and these correspond to the peaks B–G observed by Nilsson *et al.*[4,39] on cesiated Au. The fact that the same structure is observed in different laboratories and on both cesiated and sodiated samples is encouraging. It is observed that peak 2 splits off from peak 1 somewhere near $\hbar\omega = 9.0$ eV.

A selection of second-derivative energy spectra taken on cesiated Au is shown in Fig. 15. The peaks numbered 1–6 are seen once again, but the sharper resolution of the higher-derivative curves enables us to see more detail. The splitting of peak 2 from peak 1 is clearly evident. The doublet composed of peaks 3 and 4 undergoes some changes in profile and gradually fades away at the higher photon energies. Peak 5 also undergoes some profile changes and is observed to have a shoulder on its low-energy side at some photon energies. Peak 6 is also interesting; it increases in strength quite suddenly at $\hbar\omega = 10.2$ eV and is then later split into a doublet at $\hbar\omega = 10.8$ eV.

All the effects mentioned above—namely, peaks splitting, fluctuating in strength, appearing, disappearing, etc.—are highly characteristic of direct transitions.

Theory and experiment on Au are summarized and compared in Fig. 16. The smooth curves are the peak loci in the EDJDOS based on Ballinger and Marshall's nonrelativistic bands[19] as outlined in Sec. IIB. It is seen that the agreement is not as good as for Cu and Ag. The numbers in Fig. 16

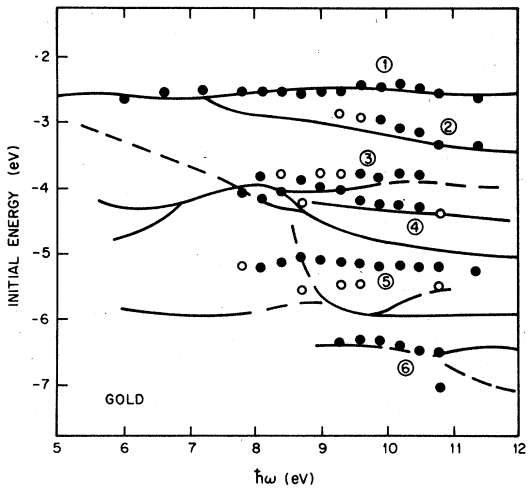

FIG. 16. Structure plot for Au comparing peak positions in the experimental spectra (full and open circles) with peak loci in the theoretical EDJDOS (smooth curves).

are associated with the experimental points. It is seen that experimental peaks 1 and 2 fall close to theoretical curves which do diverge from a single curve at low photon energies. Experimental peak 6 also falls close to a theoretical curve with which it could possibly be identified. However, the correspondence between theory and experiment in the intermediate d-band region is not so encouraging. It is possible that experimental peak 5 is associated with the theoretical curve 0.6–0.8 eV lower down in energy. It is also possible that peaks 3 and 4 are associated with two of the three theoretical curves with whose energy range they overlap. In view of the strong likelihood of large relativistic effects which have been completely neglected here, it would be dangerous to make any definite identifications. It is felt that the modest measure of agreement between experiment and theory shown in Fig. 16 is about as good as can be expected from a nonrelativistic band calculation.

V. CONDUCTION-BAND-TO-CONDUCTION-BAND TRANSITIONS

A direct-transition effect observed and identified by Berglund and Spicer[1] in their early work on Cu and Ag was due to transitions from the conduction-like bands between the top of the d bands and the Fermi level to a higher-lying conduction band. These transitions start near $L_{2'} \rightarrow L_1$ and spread to other parts of the zone on increasing $\hbar\omega$. They manifest themselves as a peak which appears at the high-energy end of the EDC and then moves to lower initial energies on increasing $\hbar\omega$. This observation has been confirmed in our new experiments on Cu and Ag and has been seen also in sodiated Au. Nilsson *et al.*[39] have observed the same transition in cesiated Au. The effect is illustrated in Fig. 17, where we show the high-energy end of some of the EDC's measured in this work on all three metals.

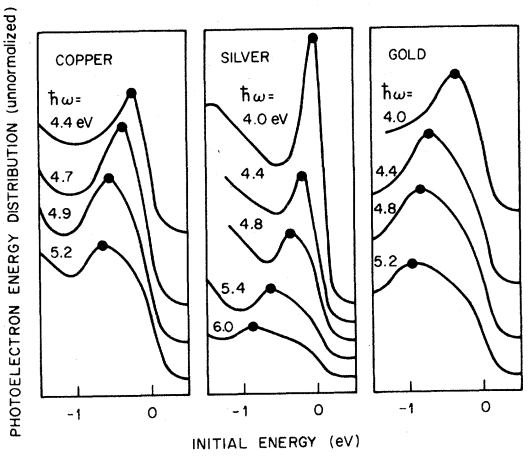

FIG. 17. High-energy end of the EDC's on Cu, Ag and Au taken at low photon energies on low work function samples.

By examining the band structure along the ΓL symmetry direction, Berglund and Spicer[1] were led to suppose that the contribution to the EDC from such transitions would consist of a narrow sharp peak which they then identified with the observed peak. A more recent analysis of the problem by Koyama and Smith[23] shows that the apparent peak really corresponds to the low-energy edge of a rectangular-box-shaped contribution to the EDJDOS. In fact, the locus of this edge is plotted as the line L in Fig. 3 and is discussed in Sec. II C.

Since the d bands are not involved in these transitions, we may dispense with the combined interpolation scheme and use a simple two-band model. Koyama and Smith[23] show that, in this approximation the locus of the low-energy edge is given by

$$E_{\min} = [(\hbar\omega - E_G)^2 - 4V_G^2]/4E_G \ . \tag{10}$$

E_G equals $(\hbar^2/2m)G^2$, where $\vec{G}$ is one of the $\langle 111 \rangle$ reciprocal-lattice vectors; V_G is the Gth Fourier component of a pseudopotential. For the purposes of fitting the bands we put $2V_G$ equal to the $L_{2'} \rightarrow L_1$ band gap, which is known to be 4.2, 4.2, and 3.5 eV in Cu, Ag, and Au, respectively.[15,16] The curve of $E_{\min}$ vs $\hbar\omega$ must pass through the energy of the $L_{2'}$ point when $\hbar\omega = 2V_G$. We place $L_{2'}$ at 0.7, 0.3, and 0.5 eV below the Fermi level in Cu, Ag, and Au, respectively.[43] These values are consistent with those quoted elsewhere[14] and are found to give reasonable results for the radii of the Fermi-surface necks (see Appendix). The values for E_G calculated from the lattice constants are 34.6, 27.0, and 27.2 eV for Cu, Ag, and Au, respectively. The parameters for computing Eq. (10) are therefore completely specified and the curves are plotted in Fig. 18. The circles represent the locations of the peaks in the experimental EDC's and are found to fall at energies slightly greater than the line for $E_{\min}$. This is not surprising since the true location of the edge probably occurs somewhere on the slope at energies below the peak rather than at the peak itself.

In Cu and Au the experimental points do not extend too far since the peak quickly becomes obscured by the d-band structure. In Ag, where the d bands are much lower, the conduction-band-to-conduction-band peak can be followed over a much wider range of photon energy. An interesting effect seen in Fig. 17 is the sharpness of the direct-transition peak in Ag at the lowest photon energies compared with the other metals. This has given rise to some speculation concerning the possibility of many-body resonances.[44] However, we see

from Fig. 18 that at its onset the peak is predicted to be narrower in Ag than in Cu or Au. The sharpness of the peak in Ag may be merely an indication that $L_{2'}$ is significantly closer to the Fermi level than in the other metals. It is suggested, therefore, that there is no clearcut evidence for a many-body effect.

In Au, it is evident from the data in Figs. 17 and 18 that the separation between $L_{2'}$ and L_1 cannot be greater than about 4 eV. Our EDC's and those of Nilsson *et al.*[39] on cesiated Au tend to confirm the value of 3.5 eV deduced from modulated optical studies[15] and alloy reflectance work.[16] We conclude that the value of 6.0 eV calculated by Ballinger and Marshall[19] and the value of 8.0 eV proposed by Krolikowski and Spicer[6] are far too high. Krolikowski and Spicer's estimate was based on an entirely different piece of structure. It occurs between the d bands and the Fermi level and is labeled A in Fig. 14. The more recent work therefore indicates that their tentative assignment was incorrect.

At photon energies below the $L_{2'} - L_1$ threshold we still observe photoelectrons all the way up to the high-energy end of the EDC's as determined by the Fermi level. No direct transitions are permitted in this energy range. Experiments were performed on cesiated Cu at liquid-nitrogen temperature and showed that the EDC's were insensitive to temperature, indicating that indirect (phonon-assisted) transitions can be ruled out. The transitions must therefore be categorized as nondirect.

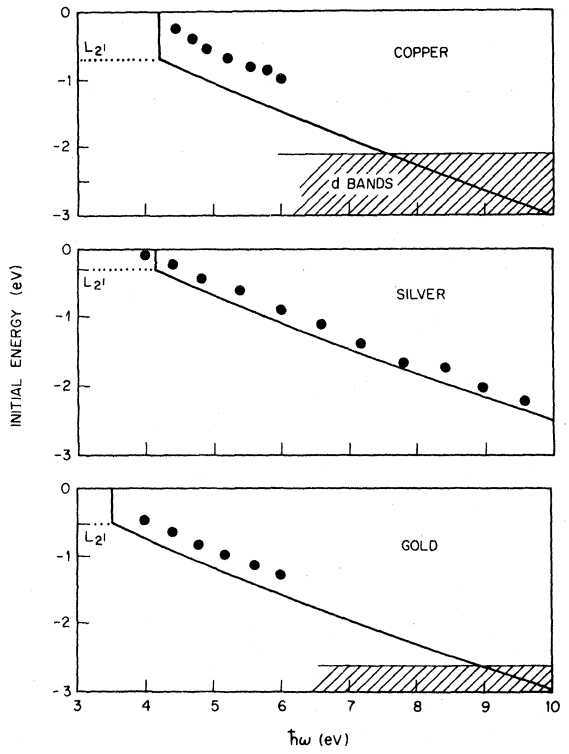

FIG. 18. Structure plots comparing the peak positions indicated in Fig. 17 with the loci of the low-energy edge for conduction-band-to-conduction-band transitions.

VI. CONCLUSIONS

The main conclusion of the present work has been the successful interpretation of the photoelectron energy spectra from Cu, Ag, and Au in terms of direct transitions. This is in contrast to early work where it was concluded that optical transitions in the noble metals are predominantly nondirect.[1,6] The experimental spectra reported here and in recent work at other laboratories[4,5] show numerous instances of characteristically direct behavior (i.e., peak splittings, abrupt appearances, and disappearances of peaks, etc.). Apart from these purely qualitative observations, we have seen good correlation between energy locations of peaks in the experimental spectra and peak loci in the EDJDOS calculated numerically from model band structures. This lends further support to the direct-transition interpretation. A corollary of the main conclusion is the success of one-electron band theory whose validity has been tactily assumed throughout.

The phenomenological aspect of the nondirect model consists of unfolding the experimental EDC's to obtain an "optical density of states."[2,6] The resemblance of the optical DOS's to calculated band DOS's has proved to be a valuable guide to band theorists. Expanding the experimental energy range, either upwards[5] or downwards,[3,4] reveals effects which cannot be accommodated in the nondirect model. The present work suggests that a more reliable way of determining the density of states is to find a band structure whose EDJDOS is consistent with the photoelectron energy spectra and then to compute the DOS from the band structure. The DOS's computed from the band structures used in the calculations described above are shown in Fig. 19. The DOS's for Cu and Ag are regarded as quite reliable. In view of the poorer agreement between the EDJDOS and the experimental spectra, the density of states for Au is not so reliable, although it is probably as good as one can do with a nonrelativistic band structure.

We place the upper *edge* of the d-band contribution to the DOS's at 2.0, 4.0, and 2.35 eV below the Fermi level in Cu, Ag, and Au, respectively. The uppermost d-band *peak* is placed, respectively, at 2.15, 4.3, and 2.7 eV below the Fermi level. These locations are slightly nearer to the Fermi level than in some of the other photoemission investigations. This is a consequence of the method of determining the Einstein cutoff discussed in Sec. III A. Placing the top of the d band any lower

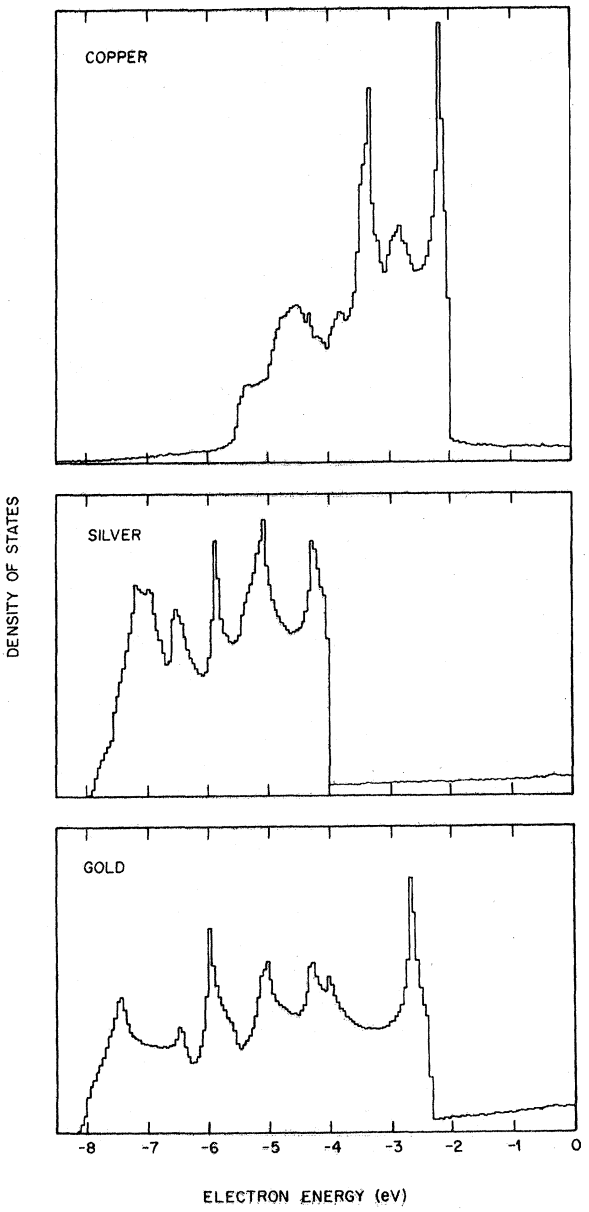

FIG. 19. Densities of states for Cu, Ag, and Au computed from the interpolated band structures. The zero of energy is taken at the Fermi level.

would raise the frequency of the fundamental edge in the theoretical ϵ_2 shown in Fig. 4. Our model band structures have, however, been able to fit simultaneously the position of the uppermost d peak in the photoelectron spectra and the edge in ϵ_2. This provides another reason for preferring our choice for the location of the Einstein maximum.

The emphasis in this paper has been on the existence and energy location of structure both in theory and experiment. No serious attempt has been made to predict the exact shape and magnitude of the EDC's. This would be a difficult task – involving, as it does, knowledge of momentum matrix elements, electron-electron scattering strengths, angular anisotropies, crystal orientation effects, surface transmission coefficients, etc. In addition, there are possible processes which could occur during the optical excitation event and cause a breakdown of strict conservation of one-electron $\vec{k}$ vector; electron-electron scattering and localization of the hole have been proposed in this context.[2,45] Such processes may indeed occur. For example, it has never been demonstrated that the broadening in the experimental EDC's is due entirely to finite instrumental resolution. The $\vec{k}$-violating processes may cause a smearing and may contribute to the background of the EDC's.[45] They do not seem to destroy the applicability of a direct-transition interpretation of the structure. The experimentalist interested in band-structure effects is more or less obliged to concentrate on the location of the structure in the spectra until some of the theoretical questions have been resolved. Much use has been made in this paper of higher-derivative spectra which have the effect of picking out the structure and discarding the background. It may be that in taking the higher-derivative spectra we are doing precisely what is required to isolate the volume contribution and the one-electron band-structure effects.

The procedure described here has been to compare experimental spectra with the predictions of model band structures. Finding suitable band structures has involved an element of trial and error. The optical transitions involved in photoemission occur at general points in the Brillouin zone, and this has necessitated the use of an interpolation scheme. The currently available interpolation schemes contain about a dozen disposable parameters. An interesting question is whether these parameters could be determined entirely from the photoelectron spectra. This has not been attempted so far, but in view of the improved precision of the higher-derivative spectra, it would certainly be worth a try. We note in this regard the guidelines for empirical fitting procedures laid down by Phillips.[46] Certain combinations of the parameters are inadmissible, and the number of independent parameters can actually be reduced. It has been pointed out[46,47] that the parameters describing the form of the d bands are tied to two fundamental quantities: the width of the d resonance and the location of its center with respect to the free-electron-like s, p bands. With a reduced number of parameters, it may be possible, armed only with the photoelectron energy spectra and an interpolation scheme, to arrive at an almost purely experimental determination of the E-k curves for an arbitrary d-band metal. It

TABLE I. Energy levels at symmetry points in the model band structures. Energies are in Ry.

	Cu	Ag	Au
Γ_1	−0.10	−0.565	−0.62
$\Gamma_{25'}$	+0.299	−0.445	−0.43
Γ_{12}	+0.357	−0.355	−0.32
X_{11}	+0.163	−0.56	−0.61
X_3	+0.200	−0.555	−0.60
X_2	+0.399	−0.295	−0.235
X_5	+0.412	−0.275	−0.20
$X_{4'}$	+0.704	(+0.145)	+0.11
K_4	+0.367	−0.345	−0.30
L_{11}	+0.156	−0.535	−0.61
L_{31}	+0.297	−0.435	−0.44
L_{32}	+0.401	−0.295	−0.22
$L_{2'}$	+0.510	(−0.005)	−0.06
L_{12}	+0.853	(+0.295)	(+0.24)
E_F	+0.560	+0.020	(−0.025)

TABLE II. Parameters of the interpolation scheme used in numerical calculations.

α	0.01531	0.01461	0.01383
β	−0.10000	−0.56500	−0.62000
V_{111}	0.12500	0.14115	0.10387
V_{200}	0.17600	0.22487	0.15516
E_0	0.33075	−0.38750	−0.35750
Δ	−0.00445	−0.01990	−0.02512
A_1	0.02031	0.02813	0.03938
A_2	0.00619	0.00688	0.01063
A_3	0.01025	0.01623	0.02003
A_4	0.01295	0.02060	0.02628
A_5	0.00262	0.00375	0.00531
A_6	0.00826	0.00985	0.01708
B_1	0.4125	0.60	0.57
B_2	1.00	0.56	1.16

seems likely that further developments in the use of photoemission as a means of determining band structure will go hand in hand with developments in the use of interpolation schemes.

ACKNOWLEDGMENTS

I am grateful to M. M. Traum for his assistance with the experiments and to L. F. Mattheiss for helpful conversations in the early stages of the calculations. Thanks are due also to K. K. Thornber and J. L. Shay for critical readings of the manuscript. Finally, I am indebted to Professor W. E. Spicer for introducing me to the interesting problem of photoemission from metals.

APPENDIX

Listed here are the parameters of the interpolated band structures used in the numerical calculations described in Sec. II. The interpolation scheme used was that due to Hodges, Ehrenreich, and Lang.[12]

Table I shows the energies at the symmetry points Γ_1, $\Gamma_{25'}$, Γ_{12}, X_{11}, X_3, X_2, X_5, $X_{4'}$, L_{11}, L_{31}, L_{32}, $L_{2'}$, and L_{12}. The position of the Fermi level E_F on the same energy scale is also shown. The values in parentheses are values which have been adjusted by the author. All energies are in Ry.

In Ag, Ballinger and Marshall's[19] values for $L_{2'}$, L_{12}, $X_{4'}$, and E_F were all raised by 0.020 Ry. This is equivalent to a rigid downward shift of the d-band complex with respect to the free-electron s, p bands. This small adjustment appears to be quite consistent with the guidelines laid down by Phillips.[46]

In Au, Ballinger and Marshall's value for E_F was lowered by 0.025 Ry. This is equivalent to a small rigid raising of the d bands. The level L_{12} was lowered by 0.14 Ry. This was considered necessary in order to bring the $L_{2'} - L_{12}$ band gap in reasonable agreement with the optical value. This adjustment is quite important for another reason. In the procedure used here for fitting the interpolation scheme, the position of the upper unfilled bands is determined largely by where one chooses to place L_{12}. This therefore influences the frequencies of the permitted optical transitions all over the zone. In view of this large arbitrary adjustment, and also the neglect of large relativistic effects, the band structure used here for Au must be regarded with greater caution than that for Cu or Ag.

The parameters of the interpolation scheme are shown in Table II. The values for Cu are taken from Hodges *et al.*[12,20] The values for Ag and Au were deduced by the author by fitting the energy levels listed in Table I using a method described by Hodges.[20] The reader is referred to the original papers by Hodges *et al.* for an explanation of the symbols. Very briefly, the parameters α, β, V_{111}, and V_{200} specify the four-OPW part of the band structure; E_0, Δ, A_1, A_2, A_3, A_4, A_5, and A_6 specify the tight-binding d bands; B_1 and B_2 are parameters which simulate the effects of hybridization.

The radii of the Fermi-surface necks given by these band structures are 0.20, 0.19, and 0.17 expressed in units of the free-electron Fermi radius for Cu, Ag, and Au, respectively. The experimental values from de Haas–van Alphen[48] and magnetoacoustic[49] experiments are 0.19, 0.14, and 0.18, respectively. Within the energy resolution of photoemission experiments (≈0.1 eV), the Fermi-surface agreement may be regarded as good.

[1]C. N. Berglund and W. E. Spicer, Phys. Rev. 136, A1030 (1964); 136, A1044 (1964).

[2]W. E. Spicer, Phys. Rev. 154, 385 (1967).

[3]N. V. Smith, Phys. Rev. Letters 23, 1452 (1969).

[4]P.-O. Nilsson, C. Norris, and L. Walldén, Solid State Commun. 7, 1705 (1969).

[5]D. E. Eastman and J. K. Cashion, Phys. Rev. Letters 24, 310 (1970).

[6]W. F. Krolikowski and W. E. Spicer, Phys. Rev. 185, 882 (1969); Phys. Rev. B 1, 478 (1970).

[7]W. E. Spicer, Phys. Rev. 125, 1297 (1962).

[8]N. V. Smith and M. M. Traum, Phys. Rev. Letters 25, 1017 (1970).

[9]G. W. Gobeli, F. G. Allen, and E. O. Kane, Phys. Rev. Letters 12, 94 (1964).

[10]See, for example, M. Cardona, in *Solid State Physics*, edited by F. Seitz, D. Turnbull, and H. Ehrenreich (Academic, New York, 1969), Suppl. 11.

[11]F. M. Mueller and J. C. Phillips, Phys. Rev. 157, 600 (1967).

[12]L. Hodges, H. Ehrenreich, and N. D. Lang, Phys. Rev. 152, 505 (1966).

[13]F. M. Mueller, Phys. Rev. 153, 659 (1967).

[14]H. Ehrenreich and H. R. Phillipp, Phys. Rev. 128, 1622 (1962); B. R. Cooper, H. Ehrenreich, and H. R. Phillipp, *ibid.* 138, A494 (1963).

[15]M. Garfinkel, J. J. Tiemann, and W. E. Engeler, Phys. Rev. 148, 695 (1966).

[16]D. Beaglehole and E. Erlbach, Solid State Commun. 8, 255 (1970).

[17]G. A. Burdick, Phys. Rev. 129, 138 (1963).

[18]E. C. Snow, Phys. Rev. 172, 708 (1968).

[19]R. A. Ballinger and C. A. W. Marshall, J. Phys. C 2, 1822 (1969).

[20]L. Hodges, thesis, Harvard University, 1966 (unpublished); H. Ehrenreich and L. Hodges, in *Methods in Computational Physics*, edited by B. Alder, S. Fernbach, and M. Rothenberg (Academic, New York, 1968), Vol. 8, p. 149.

[21]F. M. Mueller, A. J. Freeman, J. O. Dimmock, and A. M. Furdyna, Phys. Rev. B 1, 4617 (1970).

[22]D. Brust, Phys. Rev. 139, A489 (1965).

[23]R. Y. Koyama and N. V. Smith, Phys. Rev. B 2, 3049 (1970).

[24]E. O. Kane, Phys. Rev. 175, 1039 (1968).

[25]N. V. Smith and W. E. Spicer, Opt. Commun. 1, 157 (1969).

[26]N. W. Ashcroft and W. L. Schaich, in Proceedings of the Electronic Density of States Symposium, National Bureau of Standards, Washington, D. C., 1969 (unpublished); and (private communication).

[27]W. E. Spicer, Phys. Rev. Letters 11, 243 (1963). It is generally added that other characteristically direct-transition behavior (abrupt appearances and disappearances of peaks, fluctuations in peak strength) must also be absent before transitions can be designated as nondirect; see W. E. Spicer and G. J. Lapeyre, Phys. Rev. 139, A565 (1965); the way in which nondirect transitions are identified has been precisely defined by K. K. Thornber, Sci. Progr. (London) 57, 149 (1969).

[28]A similar result has been obtained in calculations on Pd by J. F. Janak, D. E. Eastman, and A. R. Williams, Solid State Commun. 8, 271 (1970).

[29]G. Dresselhaus, Solid State Commun. 7, 419 (1969).

[30]U. Gerhardt, Phys. Rev. 172, 651 (1968); see also the discussion between J. C. Phillips, *ibid.* 187, 1175 (1969), and D. H. Seib and W. E. Spicer, *ibid.* 187, 1176 (1969).

[31]E. O. Kane, J. Phys. Soc. Japan Suppl. 21, 37 (1966).

[32]G. D. Mahan, Phys. Rev. Letters 24, 1068 (1970); Phys. Rev. B 2, 4334 (1970).

[33]L. Sutton, Phys. Rev. Letters 24, 386 (1970).

[34]W. E. Spicer and C. N. Berglund, Rev. Sci. Instr. 41, 252 (1970).

[35]L. W. James, R. C. Eden, J. L. Moll, and W. E. Spicer, Phys. Rev. 174, 909 (1968).

[36]M. M. Traum and N. V. Smith (unpublished).

[37]T. H. DiStefano and D. Pierce, Rev. Sci. Instr. 41, 180 (1970).

[38]D. E. Eastman (private communication).

[39]P.-O. Nilsson, C. Norris, and L. Walldén, Physik Kondensierten Materie 11, 220 (1970).

[40]N. V. Smith, in Ref. 26.

[41]T. A. Callcott and A. U. MacRae, Phys. Rev. 178, 966 (1969).

[42]L. Walldén, Phil. Mag. 21, 571 (1970).

[43]In a previous analysis, Berglund and Spicer (Ref. 1) place $L_{2'}$ in Cu at 0.35 eV below E_F rather than the 0.7 eV quoted here. Their assignment is based on a peak in the EDC's which is attributed to nondirect transitions from the region of high density of states near $L_{2'}$. This peak, however, is difficult to distinguish from peaks which arise due to the usual rounding off of the leading edge. The present writer feels that the locations of $L_{2'}$ quoted above for Cu, Ag, and Au are not inconsistent with photoemission data.

[44]J. C. Phillips, Phys. Rev. 137, A1835 (1965).

[45]S. Doniach Phys. Rev. B 2, 3898 (1970).

[46]J. C. Phillips, Advan. Phys. 17, 79 (1968).

[47]V. Heine, Phys. Rev. 153, 673 (1967).

[48]D. Shoenberg, Phil. Trans. Roy. Soc. London 255, 85 (1962).

[49]H. V. Bohm and V. J. Easterling, Phys. Rev. 128, 1021 (1962).